

Investigations on acoustic radiation by hearing aid tubes

dr. ir. Erwin Kuipers¹ and Nils Westhausen²

¹*Sonova AG, Science & Technology, CH-8712 Stäfa, Email: erwin.kuipers[at]sonova.com*

²*Jade Hochschule, Institut für Hörtechnik und Audiologie, D-26121 Oldenburg, Email: nils.westhausen[at]student.jade-hs.de*

Introduction

People with a severe to profound hearing loss need high power hearing aids. Typically these are behind-the-ear (BTE) hearing aids from which the generated sound is transmitted by a sound tube to the ear-piece. As gains exceeding 80 dB are realized, such hearing aids are susceptible to feedback instabilities. Amongst other paths, see Fig. 1, one possible feedback path is acoustic radiation by the sound tube (green arrow). In the present work, this path is investigated.



Figure 1: Behind-the-ear hearing aid, hook, tube and 3 typical feedback paths.

Theory

As a first approximation, it is assumed that the wavelength is much larger than the length of the tube, i.e. the tube is considered to be subjected to an uniformly distributed internal pressure P . The deformation of such a tube can be calculated analytically. The radial displacement U_r is given by [1, p. 683]:

$$U_r = \frac{2P}{E} \frac{r_1^2 r_2}{r_r^2 - r_1^2}, \quad (1)$$

where E is the modulus of elasticity or Young's modulus, P the internal pressure, r_1 the inner radius, and r_2 the outer radius. By defining the ratio of the outer and inner radii $K = r_2/r_1$, and transforming Eq. 1 can be expressed as:

$$U_r(\omega) = \frac{P(\omega)}{E} \frac{2r_2}{K^2 - 1}. \quad (2)$$

This equation is valid for a tube with free ends. In case both ends are longitudinally fixed, Eq. 2 has to

be multiplied by a factor $(1 - \nu^2)$ to account for the stiffening effect of the fixation. Note that doing so never leads to more than a 25% reduction in radial displacement, as $\nu \leq 0.5$.

In the frequency domain, the radial vibration velocity $V_r = i\omega U_r$, so that the volume velocity of an uniformly vibrating tube with radiating length L_{rad} becomes:

$$Q(\omega) = 4i\pi\omega L_{\text{rad}} \frac{P(\omega)}{E} \frac{r_2^2}{K^2 - 1}. \quad (3)$$

However, for visco-elastic materials, the E-modulus is not constant but depends on frequency, as are the damping losses. The shear modulus is therefore assumed to be complex:

$$G(\omega) = G_{\text{R}}(\omega) [1 + i \tan \delta(\omega)], \quad (4)$$

where G is the complex shear modulus, $G_{\text{R}}(\omega)$ is its real part, and δ the loss angle. The E-modulus can be calculated from the shear modulus with the Poisson's ratio ν :

$$E(\omega) = G(\omega)(1 + 2\nu). \quad (5)$$

As the longitudinal wave propagation velocity is defined as the square root of the E-modulus and the density:

$$c(\omega) = \sqrt{\frac{E(\omega)}{\rho}}. \quad (6)$$

It follows that the complex wavenumber k becomes:

$$k = k_{\text{R}}(1 - i\eta), \quad (7)$$

where k_{R} is the real part of the complex wavenumber, $\eta = \frac{\tan \delta}{2}$ is a dimensionless constant, and the explicit dependency on ω has been dropped for readability. Accordingly, the amplitude of a propagating plane wave will diminish with a factor $\exp(-\eta k)$ per unit length.

Tube dynamics experiments

In a first step, the structural dynamics of various tubes was investigated by means of a contact-less vibration velocity (laser-doppler vibrometer, LDV) measurement with the setup shown in Fig. 3. Herein, the tube is acoustically driven on one side by means of a hearing aid receiver. At the other end, a 2 cm³-coupler acc. IEC-711 [2] is connected. The acoustic pressure inside the coupler is measured with a microphone. In addition, the pressure at the midpoint of the tube is measured by means of a probe tube microphone. The tube is bonded to the supporting steel block with a line of adhesive so that the vibration amplitude is doubled.

Several solutions such as special paints/coatings to optimize the reflected optical signal were evaluated, however, only retro-reflective tape provided sufficient signal quality over a wide frequency range. A line of such tape was therefore carefully attached to the upper side of the tube.

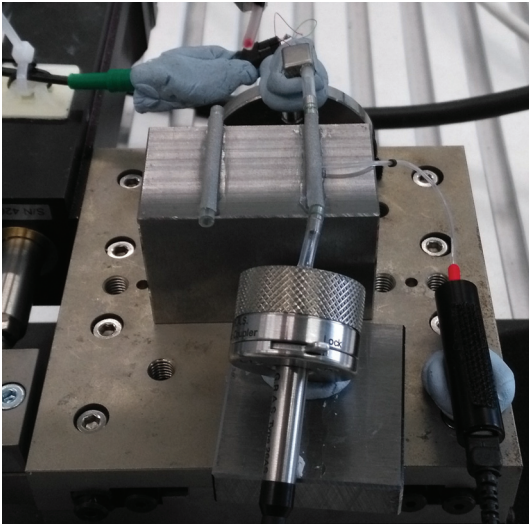


Figure 2: Setup for measuring tube vibrations.

By a first measurement, the structural response of the midpoint of the tube was evaluated against the midpoint pressure. Figure 3 shows the results expressed as transfer functions. The blue curve is the acoustic pressure predicted with an analogue network simulation (Spice). The red curve represents the measured acoustic pressure, and the yellow curve represents the displacement calculated from the laser-doppler vibration velocity measurement.

The predicted acoustic pressure is in good agreement with the measured pressure. The largest deviations are present at the acoustic resonances. At high frequencies, some frequency mismatch is notable. Such mismatch is likely caused by small differences between the simulated and the real geometry.

Secondly, the vibration amplitude curve agrees well with both other curves. The vibration displacement curve was manually fitted to the other curves by adding 211 dB. At this stage, the scaling does not have the

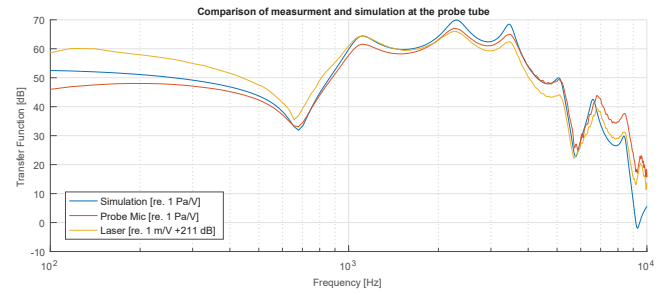


Figure 3: Magnitude of transfer function (receiver voltage to acoustic pressure) along with the scaled transfer function receiver voltage to vibration displacement.

purpose of determining the mechanical properties of the tube, but only serves as a comparison between the pressure and the structural response. From this comparison, one can conclude that a) mechanical resonances are absent and b) that the tube wall behaves spring-like.

One can see that the scaled vibration displacement curve rises above the pressure curves at low frequencies and decreases below the measured pressure curve at high frequencies. I.e. the tube wall seems to behave more rigidly at high frequencies than it does at low frequencies. This behavior is well known from visco-elastic materials. In the following, the mechanical characterization of the tube material is discussed.

Experimental characterization of tube materials

To determine the frequency-dependent E-modulus and loss angle, vibration experiments were carried out. Tubes of different lengths were attached to a vibration shaker and driven on one side. By means of an laser-doppler vibrometer the vibration velocity at the base and at the top of the tube were measured. The transfer function between the vibration velocity at the bottom and at the top for this setup is given by:

$$H_{bt} = \frac{1}{\cos kL}, \quad (8)$$

where L is the length of the tube, and the structural wavenumber k is complex as defined in Eq. 7. By performing measurements for tubes with different lengths, and fitting the resonance peaks, the E-moduli were determined. Further experiments were undertaken using a bone-conduction vibrator (BCV) as a vibration source. Figure 4 shows the results of all measurements.

One can observe that the real part of the E-modulus tends to increase with increasing frequency and that the loss angle tends to decrease. With a loss angle around 30°, vibrations in the PVC tube are strongly damped. Looking at those frequencies where multiple datapoints were measured, one notes that this measurement procedure leads to significant errors. Nevertheless, this experiment has shown that one needs to account for the

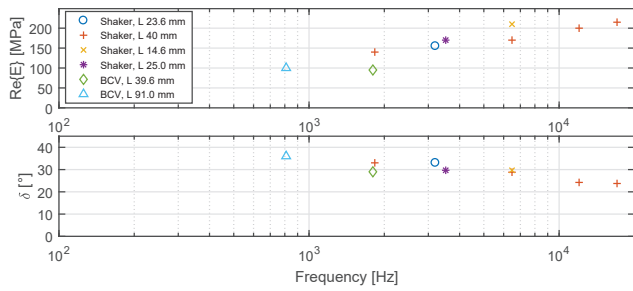


Figure 4: Real part and loss angle of the complex E-modulus for a PVC hearing aid tube determined from different tube samples.

frequency-dependent behavior when predicting the radial deformation of such tubes.

Acoustic radiation

In a further experiment the acoustic radiation of a silicone tube was investigated. This specific material was chosen in order to enhance the SNR of the acoustic measurement as the E-modulus of the silicone tube is about a factor 10 less than that of PVC. Figure 5 shows the setup. The freely exposed length of the tube equals 27 mm.

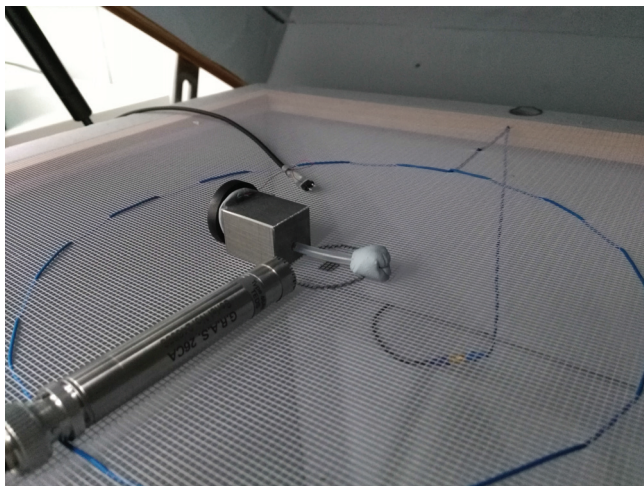


Figure 5: Setup for measuring acoustic radiation of a tube in an anechoic measurement box.

Care was taken to only expose the tube. Therefore, the receiver was acoustically insulated, see the schematic in Fig. 6

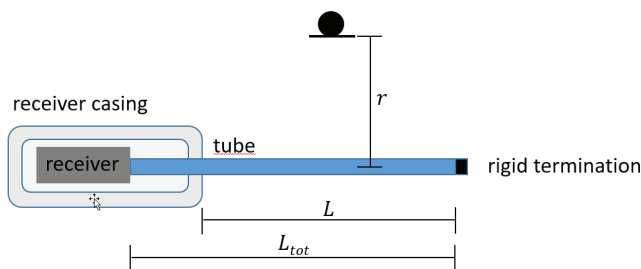


Figure 6: Schematic sketch of the setup for the acoustic radiation measurements.

The magnitude of the transfer function from receiver

voltage to the radiated acoustic pressure is shown for different distances r in Fig. 7. One can clearly see the rapid increase of radiation up to 2 kHz and the presence of two acoustic resonances in the tube. A maximum acoustic pressure of 0.3 Pa per unit Volt is reached for a distance of 5 mm, being equivalent to 84 dB SPL. For high frequencies the results are certainly influenced by scattering effects due to the presence of the receiver casing.

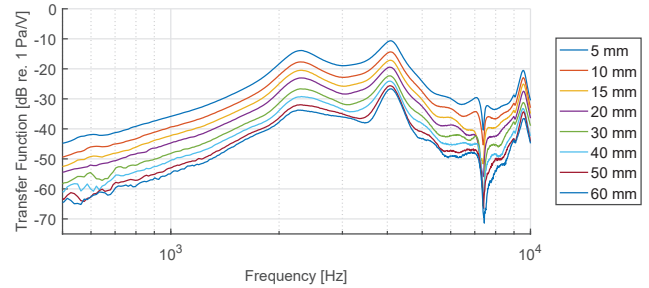


Figure 7: Magnitude of the transfer function from receiver voltage to acoustic pressure at multiple distances from the midpoint of a silicone tube.

The distinct dip between 7 and 8 kHz is caused by the presence of a pressure node at the tube midpoint, leading to a significant loss of radiation as the acoustic pressure on both sides of the node are out-of-phase.

Radiation prediction

One can employ Eq. 3 to predict the volume velocity of a radiating tube. Instead of representing the whole tube just by one monopole source, the tube is now divided into N segments. Accordingly, the acoustic radiation is modeled using N monopole sources. The acoustic pressure at distance r from the tube midpoint can then be described by:

$$P(\omega, r) = \sum_{n=1}^N \frac{i\rho\omega Q_n(\omega)}{4\pi r_n} \exp(-ikr_n) \quad (9)$$

where r_n is the distance of source n to the point of interest, $Q_n(\omega)$ is the volume velocity of tube segment n , k is the wavenumber in air. The volume velocity of each segment is calculated with a Spice simulation for the equivalent acoustic network. Figure 8 shows the field employing $N = 10$ sources for a silicone tube with a length of 27 mm. The measured acoustic field (49x50 mm, grid spacing 1 mm) is shown for comparison in Fig. 9.

The simulated acoustic field matches the measured field quite well. However, magnitude errors are present. At the acoustic resonance frequencies, these errors are most likely due to inaccuracies in the Spice simulation. Other possible errors are anisotropy of E-modulus of the tube wall, and acoustic scattering by the receiver casing. Taking $f_{sc} = \frac{c}{5L_t}$ (L_t : typical dimension) as an indicator for the frequency at which scattering sets on, scattering is expected to become noticeable from 3 kHz upwards.

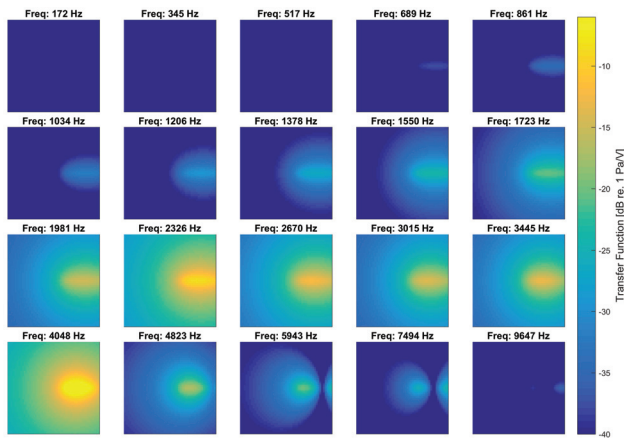


Figure 8: Simulated spatial distribution of the acoustic pressure per unit volt for a silicone tube in a free field.

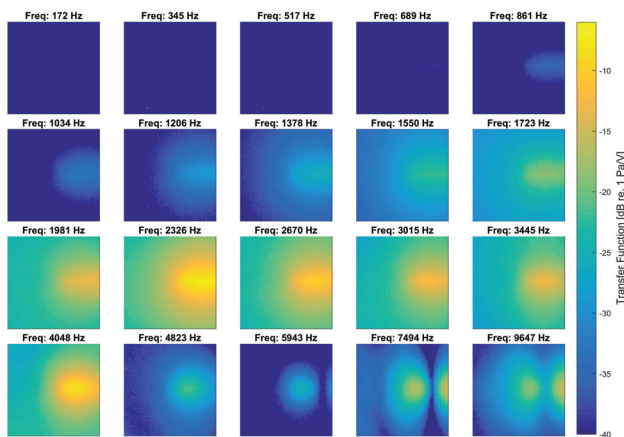


Figure 9: Measured spatial distribution of the acoustic pressure per unit volt for a silicone tube in a free field.

Feedback path prediction

The feedback (FB) threshold for a power hearing aid was predicted using 10 tube segments for three different but frequency-independent E-moduli (50, 100, 150 MPa). The prediction was performed for a BTE-configuration with an ear simulator [3]. A small vent (12x0.7 mm) in the ear-piece is assumed. As a first approximation, the radiated pressures by the tube and the vent are doubled to account for the presence of the head. The thresholds are calculated by taking the reciprocal value of the feedback path transfer functions from ear simulator pressure to microphone pressure. Figure 10 shows the thresholds due to the tube radiation and the vent. For comparison, the acoustic gain curve is shown as well. One can clearly see that the E-modulus of the tube must at least equal 100 MPa to avoid feedback instabilities. 150 MPa is preferred, to provide a sufficient stability margin.

Conclusions and outlook

The present work shows that hearing aid tubes can be characterized by a frequency-dependent complex E-modulus. However, the characterization of the used polymeric materials has to be performed with care. Analysis of the tube dynamics revealed that mechanical

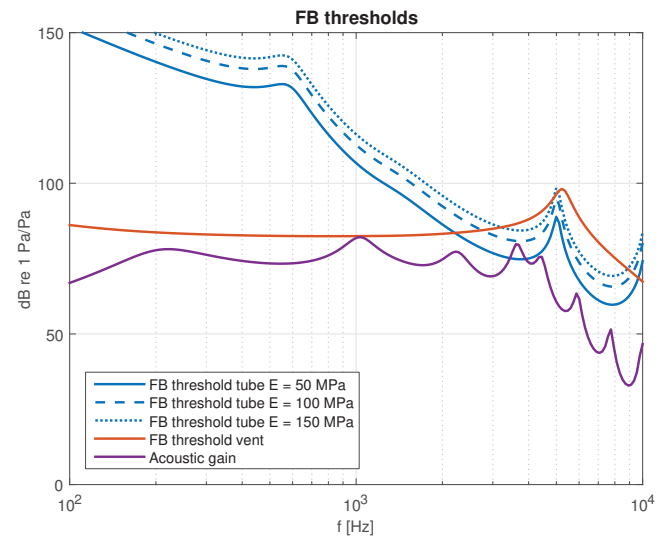


Figure 10: Predicted feedback thresholds for a hearing aid with a vent with dimensions $L \times D = 12 \times 0.7$ mm. For the tube-related feedback threshold, simulations were performed for three different E-moduli.

resonances are absent and the tube behaves spring-like with significant mechanical damping.

The predicted feedback thresholds for a power hearing aid reveal that acoustic radiation from a PVC hearing aid tube will hardly lead to acoustic feedback instabilities. However, this may change if the E-modulus in the circumferential direction is significantly lower due to anisotropy. Tube-related feedback can be avoided by sufficiently stiff tube wall design, e.g. by choosing a material with a high E-modulus or by reducing the inner tube diameter, however the latter at the cost of acoustic pressure in the ear canal at high frequencies.

It is planned to develop a more accurate measurement method for the determination of the complex E-modulus of hearing aid tubes, in particular w.r.t. radial displacement. Furthermore, in real-life applications, scattering effects by the pinna (outer ear) and the head are present. To improve the accuracy of feedback path predictions, it is therefore recommended to account for such effects, e.g. by a finite- or boundary element simulations.

References

- [1] Young, W.C. and Budynas, B., Roark's formulas for stress and strain. McGraw-Hill, 7th edition, 2002.
- [2] IEC 60118-7:2005
- [3] IEC 60318-4:2010